

APPLICATION OF A THERMOVISCOELASTIC DYNAMIC VIBRATION ABSORBER TO A NON-IDEAL OSCILLATING SYSTEM

Jorge Luis Palacios Felix, jorge.felix@unipampa.edu.br

UNIPAMPA, C. P. 07, 96412-420, Bagé, RS, Brasil

Wang Chong, wangchong@unipampa.edu.br

UNIPAMPA, 97546-550, Alegrete, RS, Brasil

José M. Balthazar, jmbaltha@rc.unesp.br

UNESP, C.P. 178, 13500-230, Rio Claro, SP, Brasil

Abstract. A dynamic vibration absorber with viscoelastic material applied to a non-ideal parametric oscillating system to suppress the Sommerfeld effect, resonance capture and jump phenomenon is studied. The absorber is a mass-bar subsystem that consists of a linear viscoelastic damping of bar type with memory in which the internal dissipative forces depend on current, deformations and its operational frequency varies with limited temperature. The non-ideal system consists of the coupling between a linear (nonlinear) oscillator and an unbalanced rotor of dc motor with limited power supply via spring connector. The numerical results show the comparison of the non-ideal system response with and without the absorber through the resonance curves and Poincaré sections. Furthermore, the suppression band of the thermoviscoelastic dynamic vibration absorber (of dynamic damping) is comparable with a conventional dynamic vibration absorber (of constant damping). For the numerical simulation was used the runge-kutta fourth-order integrator with MATLAB/SIMULINK™ applied to a six degree of freedom mathematical model of the problem in study.

Keywords: visco-elastic material, non-ideal system, dynamic vibration absorber

1. INTRODUCTION

The excitation of the vibration systems analyzed here, is taken as always limited; on the one hand by the characteristics of a particular energy source and, by other hand limited by the dependence of the motion of the vibrating system on the motion of the energy source. Note that this connection is expressed by a coupling between the differential equations of motion of the vibrating system and the source. Note, that when the excitation is not influenced by the response of a vibrating system, it is said to be an ideal energy source, or an unlimited energy sources. For non-ideal dynamical systems, one must add an equation that describes how the energy source supplies the energy to the equations that govern the corresponding ideal dynamical system. We remarked that in non-ideal systems is present the so-called **Sommerfeld effect**: steady state frequencies of the dc motor will usually increase as more power (voltage) is given to it in a step-by-step fashion. When a resonance condition with the structure is reached, the better part of this energy is consumed to generate large amplitude vibrations of the foundation without sensible change of the motor frequency. Eventually, enough power is supplied to e motor to initiate the jump, the operating frequency increases and the foundation amplitude decreases, resulting in lower power consumption by the motor.

We mention that more details on non-ideal systems theory, one can find in (Kononenko, 1969; Balthazar *et al.*, 2003), as an examples, undeserved others.

The initial implementation of vibration absorber for non-ideal systems was introduced by (Felix *et al.*, 2005a) using tuned liquid column damper. The technical of saturation phenomenon based on the 1:2 internal resonance was applied in a nonideal frame portal (Felix *et al.*, 2005b). Recently was studied linear and nonlinear electromechanical vibration absorber to reduce the Sommerfeld effect, jump phenomenon and resonance capture by (Felix and Balthazar, 2009).

Vibrating systems with purely nonlinear attachments have recently been the subject of growing interest of researchers. To a great extent, we remarked that the term energy pumping refers to the rapid and irreversible transfer of energy from a vibrating mechanical system to an attached nonlinear energy sink (NES). The occurrence of energy pumping depends on the essential nonlinearity of the sink stiffness. The concept of extracting energy away from a system in a simple fashion, so as to reduce its amplitude of vibration, is novel phenomenon and it forms the basis of concept of energy pumping(See as an example: Vakakis *et al.*, 2008). They have been shown that properly designed; essentially nonlinear local attachments may passively absorb energy from transiently loaded linear subsystems, acting in essence as (NES).

Furthermore, for the absorption of the resonance vibrations of a non-ideal structure, was introduce taking into account the coupling of a nonlinear essential oscillator (NES) to the system (Felix and Balthazar, 2009).

Felix *et al.* (2009) consider the analysis of the Sommerfeld effect of a Duffing-Rayleigh oscillator under a non-ideal excitation (unbalanced motor with limited power supply) using the method of averaging.

We announced that, a utilization of SMA spring material in ideal and non-ideal system was investigated by (Piccirillo *et al.*, 2008) and (Piccirillo *et al.*, 2009a,b), utilizing the linear optimal control technique to reduce the instability of the effect of chaotic motion.

This paper has as motivation of the work done by (Fosdick *et al.*, 1997; 1998). They investigated the reduction of the vibrations of a linear oscillator under ideal excitation, by using the device of viscoelastic dynamic vibration absorber for a limited temperature range of the viscoelastic material, especially when the main system has a fixed resonance frequency.

Next, we will adopt the following nomenclature: non-ideal oscillating system (NIS), thermo viscoelastic dynamic vibration absorber (TDVA).

2. THE PROBLEM UNDER CONSIDERATION

In Fig. 1, the NIS consists of a linear oscillator with concentrated mass m_1 with linear damping c and linear stiffness k excited by non-ideal energy source (of power limited supply) with crank shaft of radius r through of an elastic connector k_1 . When the exciter is in rotational motion clockwise $\dot{\varphi}$ from the horizontal direction φ with a known characteristic $L(\dot{\varphi}) = v_1 - v_2 \dot{\varphi}$ (where v_1 is related to the voltage applied across the armature of the dc motor and v_2 is a constant for each model of the dc motor considered) and the moment of inertia I , the linear oscillator is capable only of vertical direction x_1 .

The TDVA consists of a mass m_2 with referential elastic modulus k_e attached to the NIS through a viscoelastic bar whose intrinsic displacement is the vertical direction x_2 .

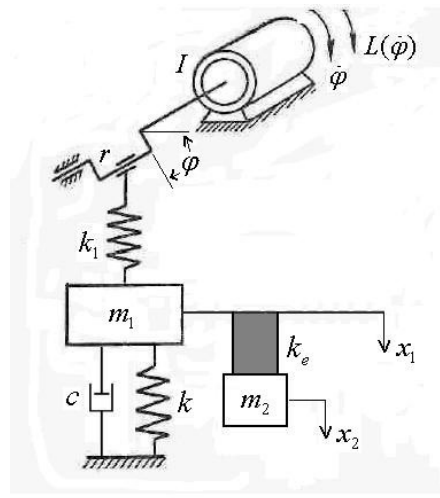


Figure 1. An approximated model of TDVA and NIS

The dynamic damping of TDVA is represented by an auxiliary function of the axial force on the particle X in the viscoelastic bar (Fosdick *et al.*, 1998).

$$\zeta(t) = \int_0^{\infty} \exp[-s/\gamma(T)] \frac{x^2(t-s) - x^2(t)}{x^2(t)} ds \quad (1)$$

where x denote the position of a particle X of the viscoelastic bar; $\gamma(T)$ is the temperature-dependent relaxation time; $\exp(\cdot)$ exponential function.

Then, the governing equation of the system is governed by the differential equations:

$$m_1 \ddot{x}_1 + c \dot{x}_1 + kx_1 = k_1 r \sin \varphi + k_e (x_2 - x_1) - \frac{G_0}{\gamma(T)} \zeta(t)$$

$$I \ddot{\varphi} = L(\dot{\varphi}) + k_1 r (x_1 - r \sin \varphi) \cos \varphi$$

$$m_2 \ddot{x}_2 = -k_e (x_2 - x_1) + \frac{G_0}{\gamma(T)} \zeta(t)$$

$$\dot{\zeta}(t) = -\frac{1}{\gamma(T)} \zeta(t) - 2 \frac{\gamma(T)}{L_0} (\dot{x}_2 - \dot{x}_1) \quad (2)$$

where L_0 is referential undistorted lengths of the viscoelastic bar; G_0 is the positive relaxation modulus.

When we consider a conventional damped dynamic vibration absorber (linear viscous-type damping) indicate as DVA, in this case $\dot{\zeta}=0$ in Eq. (2), the system DVA is

$$\begin{aligned} m_1 \ddot{x}_1 + c \dot{x}_1 + kx_1 &= k_1 r \sin \varphi + k_e (x_2 - x_1) + c_e (\dot{x}_2 - \dot{x}_1) \\ I \ddot{\varphi} &= L(\dot{\varphi}) + k_1 r (x_1 - r \sin \varphi) \cos \varphi \\ m_2 \ddot{x}_2 &= -k_e (x_2 - x_1) - c_e (\dot{x}_2 - \dot{x}_1) \end{aligned} \quad (3)$$

To simply the study of the dynamic characteristics of the TDVA-NIS, it is convenient to dimensionless the Eq. (2). Thus, we introduce a dimensionless time τ defined by $\tau = \omega_0 t$, where $\omega_0 = \sqrt{k/M}$ is the natural frequency.

Also we introduce the following dimensionless parameters: $\mu = \frac{c}{m_1 \omega_0}$, $\eta_1 = \frac{k_r r}{k L_0}$, $\eta_2 = \frac{k_r m_1 r L_0}{I k}$, $a = \frac{v_1}{I \omega_0^2}$, $b = \frac{v_2}{I \omega_0}$, $\delta = \frac{k_e}{k}$, $\eta_3 = \frac{k_r m_1 r^2}{2 I k}$, $\lambda = \frac{G_0}{k L_0}$, $\alpha = \frac{m_1}{m_2}$. Normalizing $u_1 = \frac{x_1}{L_0}$, $u_2 = \frac{x_2}{L_0}$, $u_3 = \frac{\zeta}{\gamma}$, the governing equations of motion (2), itself reduce to the following equations of the dimensionless form:

$$\begin{aligned} \ddot{u}_1 + \mu u_1 + u_1 &= \eta_1 \sin \varphi + \delta (u_2 - u_1) - \lambda u_3 \\ \ddot{\varphi} &= a - b \dot{\varphi} + \eta_2 u_1 \cos \varphi - \eta_3 \sin 2\varphi \\ \ddot{u}_2 &= -\alpha \delta (u_2 - u_1) + \alpha \lambda u_3 \\ \dot{u}_3 &= -\frac{1}{\rho} u_3 - 2(\dot{u}_2 - \dot{u}_1) \end{aligned} \quad (4)$$

where $\rho = \gamma \omega_0$ will be the control parameter of the TDVA.

Assuming $y_1 = u_1$, $y_2 = \dot{u}_1$, $y_3 = \varphi$, $y_4 = \dot{\varphi}$, $y_5 = u_2$, $y_6 = \dot{u}_2$, $y_7 = u_3$, the dynamical system (4) is written as follows

$$\begin{aligned} \dot{y}_1 &= y_2 \\ \dot{y}_2 &= -\mu y_2 - y_1 + \eta_1 \sin y_3 + \delta (y_5 - y_1) - \lambda y_7 \\ \dot{y}_3 &= y_4 \\ \dot{y}_4 &= a - b y_4 + \eta_2 y_1 \cos y_3 - \eta_3 \sin 2y_3 \\ \dot{y}_5 &= y_6 \\ \dot{y}_6 &= -\alpha \delta (y_5 - y_1) + \alpha \lambda y_7 \\ \dot{y}_7 &= -\frac{1}{\rho} y_7 - 2(y_6 - y_2) \end{aligned} \quad (5)$$

3. NUMERICAL SIMULATIONS

The numerical simulations of Eq. (5) were carried out by using ode45 of Matlab™ taken as the numerical integrator the Runge–Kutta fourth order algorithm with variable time step. The parameters selected for the simulations are shown in Table 1 while initial conditions were taken as nulls.

Table 1. Parameters and values used in the simulations

Parameters	η_1	η_2	η_3	μ	b	δ	α	λ	ρ
Dimensionless values	0.3	0.4	0.2	0.01	1.5	1.5	0.25	0.2	2.0

In Fig. 2 we plotted the oscillation amplitudes of the motor (Fig. 2a) and linear oscillator (Fig. 2b) without TDVA (in black) and with TDVA (in blue) versus the voltage (control parameter) in the range $1.2 \leq a \leq 3.4$, considering an increment $\Delta a = 0.01$ and over the dimensionless time range $0 \leq \tau \leq 3000$ during the passage through resonance region ($\varphi' \approx 1$) and only the stationary state motion.

In the range $1.5 \leq a \leq 2.5$, the angular velocity is then captured and sustained with large oscillations (due to influence of the linear oscillator response) in the natural frequency of the resonance region (Fig. 2a, in black), while one notes a large increase in the oscillation amplitude of the linear oscillator without (TDVA) (Fig. 2b, in black). When the control parameter is in the range $2.6 \leq a \leq 3.4$, before then appears a jump phenomenon on the response of the angular velocity and amplitude.

When (TDVA) is then activated, we will observe that the angular velocity of the non-ideal energy source passes through the resonance in a fast way then it presents an escape of the resonance region (in blue, Fig. 2a). Simultaneity, we observe the reduction of the amplitude of vibration of the linear oscillator (Fig. 2b, in blue).

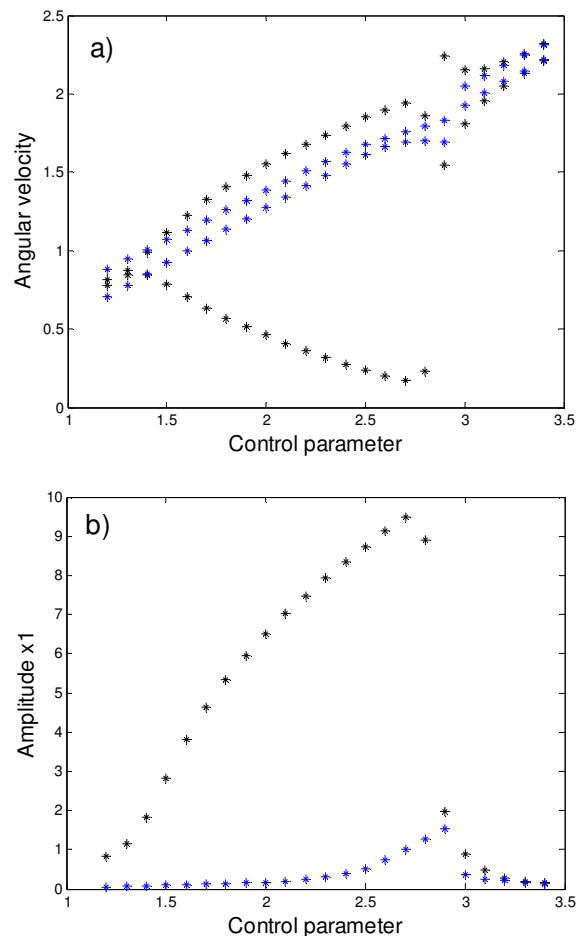


Figure 2. Resonance curve without TDVA (in black) and with TDVA (in blue): a) non-ideal motor, b) non-ideal oscillator.

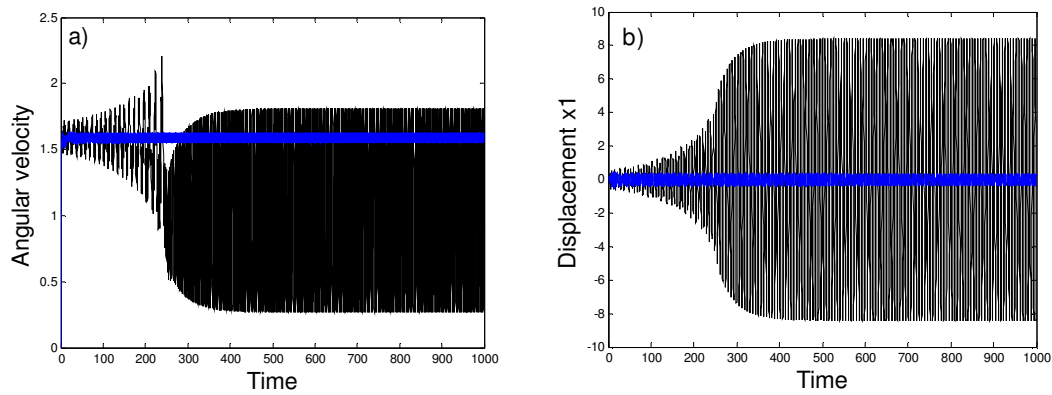


Figure 3. Simulation in the time domain of NIS without TDVA (in black) and with TDVA (in blue) for $a = 2.4$, $\rho = 2$:
 a) non-ideal source, b) non-ideal oscillator.

The Fig. 3 shows the time history for the dynamical system (5) without TDVA (in black) and with TDVA (in blue) for $a = 2.4$. This result shows the effectiveness of the TDVA in reducing the resonance capture of the non-ideal energy source and limit cycle of linear oscillator of NIS.

2.1. Performance of the TDVA

Figure 4 shows a plot of the amplitude of x_1 versus the control parameter a using the Table 1. The comparison between the oscillation amplitudes of the NIS-TDVA system (in this case, considering the dynamic damping, see Eq. (2)) and NIS-DVA (in this case, considering the constant damping, see Eq. (3)) in the range $1.2 \leq a \leq 3.4$.

Figure 5 shows a plot of the amplitude of x_1 versus the control parameter a to observe the performance of the TDVA. Clearly, the strategy of TDVA is effective in the range of $1.5 \leq a \leq 3.0$ (resonance region) when the parameter δ (elastic coefficient of TDVA) is increasing while the others parameters of Table 1 are fixed and obtaining a significant reduction of the Sommerfeld effect and the reduction of x_1 oscillation amplitude.

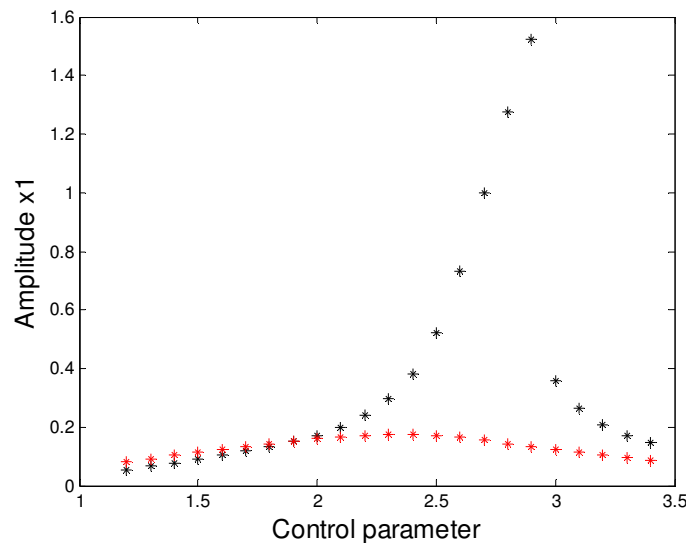


Figure 4. Resonance curve of x_1 versus a ($1.2 \leq a \leq 3.4$). Comparison between the TDVA-NIS response (in black) and the DVA-NIS response (in red).

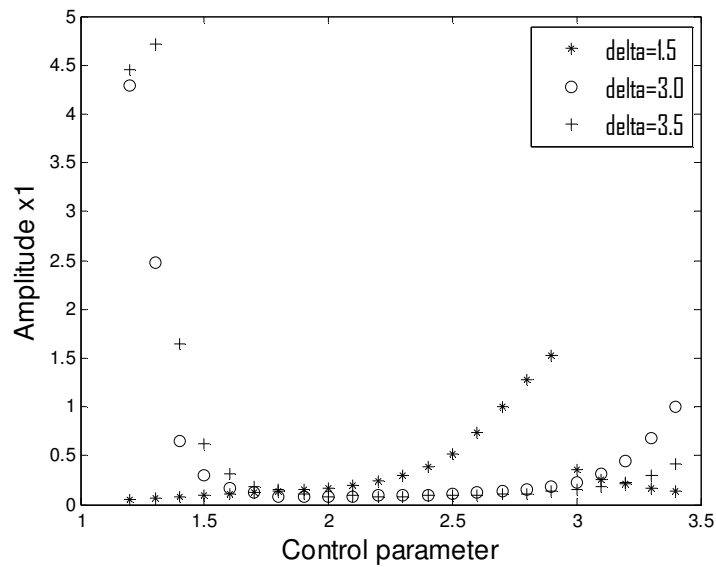


Figure 5. Simulation of Eq. (5) for $\delta=1.5$ (**); $\delta=3.0$ (oo); $\delta=3.5$ (++)

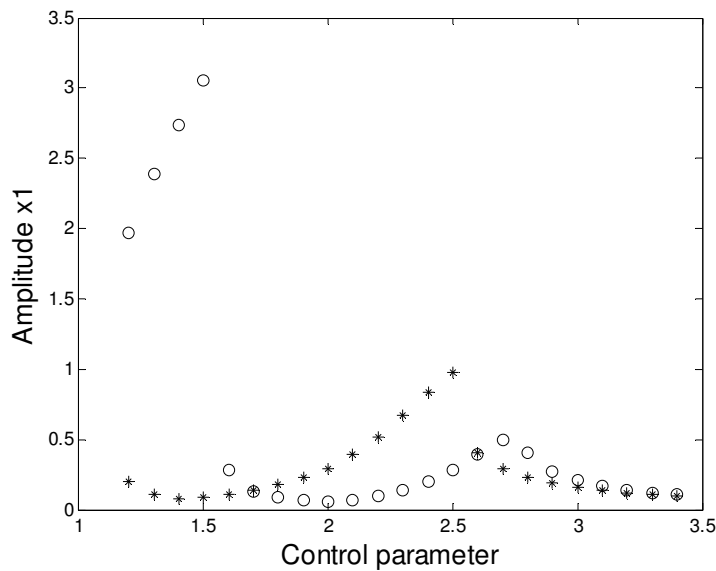


Figure 6. Simulation of Eq. (5) with $\delta=0.5$, $\alpha=1.0$ (**) and $\alpha=2.0$ (oo)

2.2. Chaotic behavior and control of the Nonlinear NIS

Hence, the nonlinear stiffness to the NIS is now focused as in (Felix *et al.*, 2009c), in this case will be Duffing-Holmes-type oscillator and we observe the effectiveness of the TDVA.

To obtain the chaotic dynamical, we implement the cubic stiffness of the form $-kx_1 + k_3x_1^3$ in the equation first of Eq. (2) and we assume parameters values $\eta_1=0.2$; $\eta_2=0.3$, $\alpha=1.25$, $k_3=0.3$ while the others are fixed. For the analysis, the control parameter of the motor was considered as $a=2.4$.

In Fig. 7, we show that the uncontrolled system (2) (NIS without TDVA) has chaotic motion (strange attractor in black). When the TDVA was activated in the system (2) we have a periodic motion (limit cycle in red). In Fig. 8 and Fig. 9 show the Poincaré section to strange attractor and to periodic attractor, respectively, for $a = 2.4$.

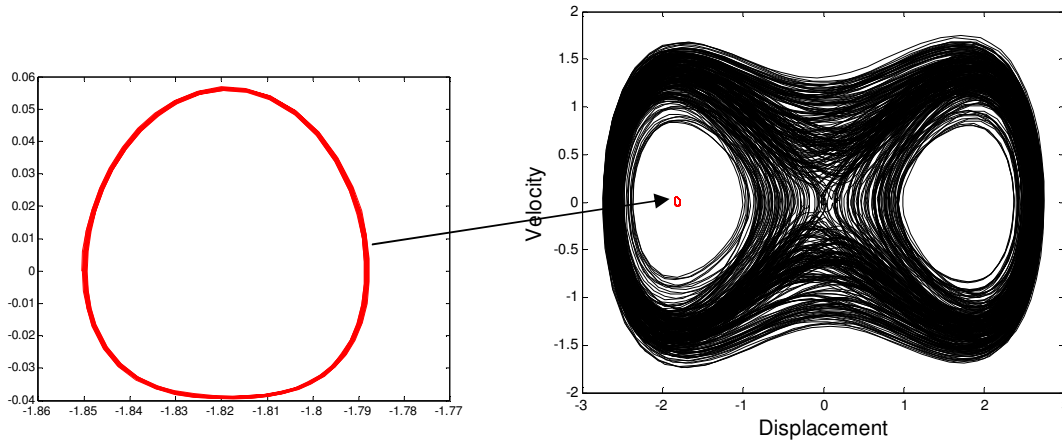


Figure 7. Phase portrait for control parameter $a = 2.4$ showing the co-existence of chaotic attractor without TDVA (in black); and limit cycle attractor with TDVA (in red).

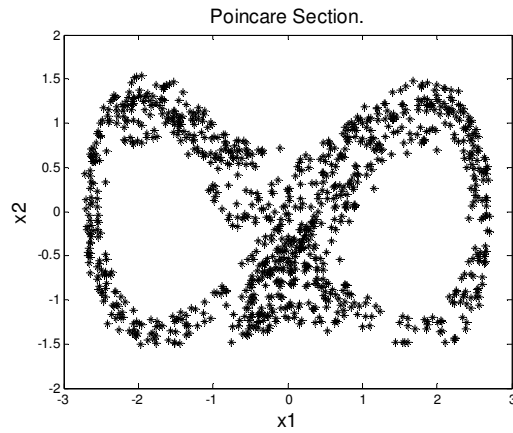


Figure 8. Poincaré section for the chaotic attractor of Eq. (2) without TDVA

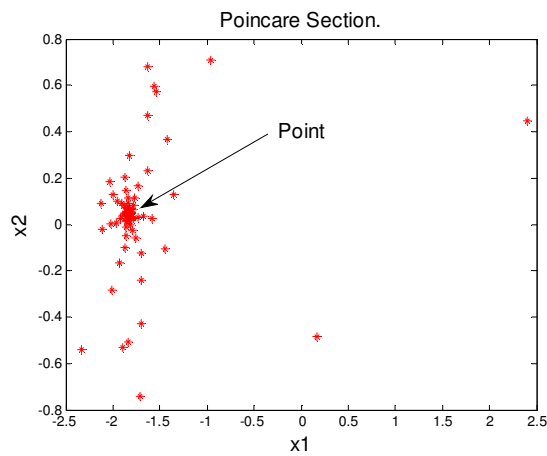


Figure 9. Poincaré section for the periodic attractor of Eq. (2) with TDVA

2.3. Numerical Results of adding nonlinear elastic modulus to the TDVA

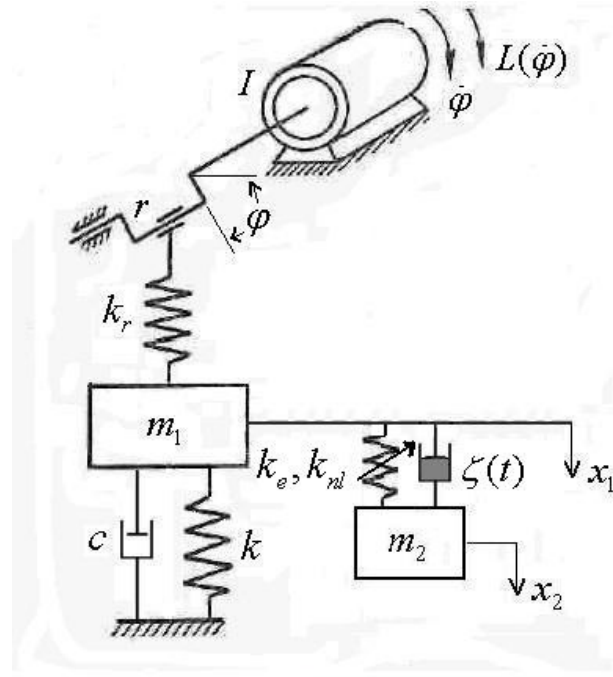


Figure 10. An approximated model of TDVA with nonlinear stiffness and NIS.

Hence, we extend Fosdick and Ketema (1998) original work, adding a non-linear stiffness to the TDVA without altering its dynamic damping characteristics, as is shown in Fig. 10. Then the Eq. (2) in its dimensionless form or Eq. (4) can be rewritten as a system of seven first order nonlinear differential equations:

$$\begin{aligned}
 \dot{y}_1 &= y_2 \\
 \dot{y}_2 &= -\mu y_2 - y_1 + \eta_1 \sin y_3 + \delta(y_5 - y_1) + \delta_1(y_5 - y_1)^3 - \lambda y_7 \\
 \dot{y}_3 &= y_4 \\
 \dot{y}_4 &= a - b y_4 + \eta_2 y_1 \cos y_3 - \eta_3 \sin 2y_3 \\
 \dot{y}_5 &= y_6 \\
 \dot{y}_6 &= -\alpha \delta(y_5 - y_1) - \alpha \delta_1(y_5 - y_1)^3 + \alpha \lambda y_7 \\
 \dot{y}_7 &= -\frac{1}{\rho} y_7 - 2(y_6 - y_2) .
 \end{aligned} \tag{6}$$

The parameters used for the simulations of Eq. (6) are shown in Table 1 while initial conditions were taken as nulls.

Figure 11 shows the reduction of the jump effect and of the oscillation amplitude x_1 from $\delta_1 = 0.0$ to $\delta_1 = 1.2$. Then the effect of the nonlinearity of elastic modulus of TDVA is predominant.

Figure 12 shows a plot of the amplitude of x_1 versus the control parameter a to observe the performance of the TDVA, with a kind nonlinear essential stiffness (NES type), in this case $\delta = 0$. In the range of $1.5 \leq a \leq 3.0$ (resonance region) we observe the effectiveness of the TDVA when the parameter has the values $\alpha = 0.5, 1.0, 2.0$ while the others parameters of Table 1 are fixed. The reduction of the oscillation amplitude of the NIS with TDVA is predominant in comparison with oscillation amplitude of Fig. 2b without TDVA.

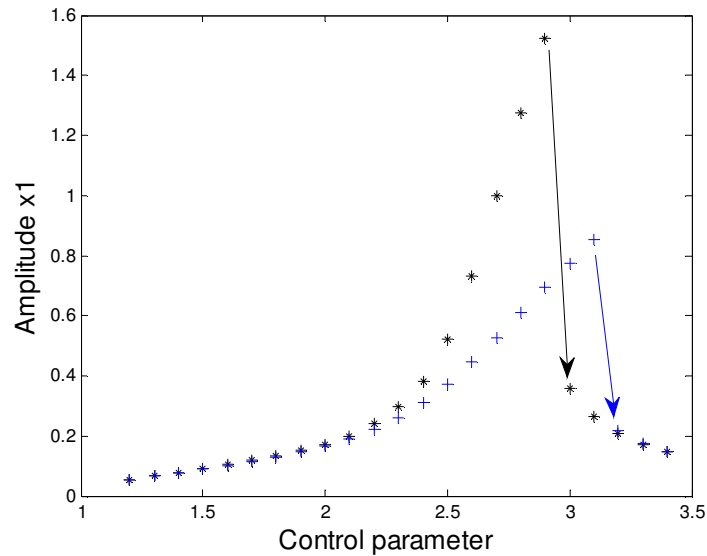


Figure 11. Simulation of Eq. (6) with $\delta_1 = 0.0$ (**) and $\delta_1 = 1.2$ (++)

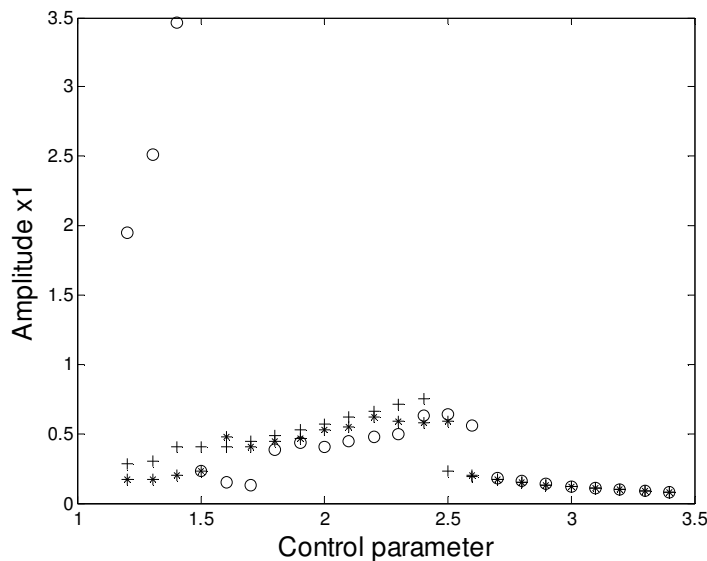


Figure 12. Simulation of Eq. (6) with $\delta = 0$, $\delta_1 = 1.2$ when $\alpha = 0.5$ (++) , $\alpha = 1.0$ (**), $\alpha = 2.0$ (oo)

3. CONCLUSIONS

The viscoelastic dynamic vibration absorber whose operational frequency varies with temperature is proposed in order to suppress resonance vibrations, Sommerfeld effect and chaotic behavior in a non-ideal oscillating system through of the numerical simulations.

This TDVA is based on the fact that the dynamic damping depending of the temperature and we compare with a linear oscillator of constant damping. The numerical results of resonance curves, Poincare section and phase portrait showed the effectiveness of the TDVA applied in the resonance passage of the NIS.

Adding a non-linear stiffness to the TDVA without altering the characteristics of the dynamic damping, we observe the effectiveness in reducing the jump effect (or Sommerfeld effect) of the NIS.

Future work will study analytical method of averaging and LQR method for nonlinear essential oscillator with dynamic damper.

4. ACKNOWLEDGEMENTS

The authors acknowledge the support of the Brazilian Agencies CNPq and CAPES.

5. REFERENCES

- Balthazar, J.M., Mook, D.T., Weber, H.I., Brasil, R.M.L.R.F., Fenili, A., Belato, D. and Felix, J.L.P., 2003. "An overview on non-ideal vibrations". *Meccanica*, Vol. 38, No. 6, pp. 613-621.
- Kononenko, V., 1969. "Vibrating Systems with Limited Power Supply", Illife Books, London.
- Felix, J.L.P., Balthazar, J.M. and Brasil, R.M.L.R.F., 2005. "On tuned liquid column dampers mounted on a structural frame under a non-ideal excitation". *Journal of Sound and Vibration* 282, pp. 1285-1292.
- Felix, J.L.P., Balthazar, J.M. and Brasil, R.M.L.R.F., 2005. "On saturation control of a non-ideal vibrating portal frame foundation type shear-building". *Journal of Vibration and Control*, 11, pp. 21-136.
- Felix, J.L. Palacios and Balthazar, J.M., 2009. "Comments on a nonlinear and non-ideal electromechanical damping vibration absorber, sommerfeld effect and energy transfer". *Nonlinear dynamics*, vol. 55, numbers 1-2, pp. 1-11.
- Felix, J.L. Palacios, Balthazar, J.M. and Dantas, J.M.H., 2009. "On energy pumping, synchronization and beat phenomenon in a nonideal structure coupled to an essentially nonlinear oscillator". *Nonlinear dynamics*, vol. 56, numbers 1-2, pp. 1-11.
- Felix, J.L.P., Balthazar, J.M. and Brasil, R.M.L.R.F., 2009. "Comments on nonlinear dynamics of non-ideal Duffing-Rayleigh oscillator: numerical and analytical approaches". *Journal of sound and Vibration*, 319, pp. 1136-1149.
- Fosdick, R.L. and Ketema, Y., 1998. "A thermoviscoelastic dynamic vibration absorber". *Journal of Applied Mechanics*, Vol. 65, pp. 17-24.
- Fosdick, R.L., Ketema, Y. and Yu, J.H., 1997. "Vibration damping through the use of materials with memory". *International Journal of Solids and Structures*, Vol. 35, pp. 5-6.
- Piccirillo, V., Balthazar, J. M., Pontes Jr., B. R. and Felix, J. L. P., , 2008. "On a nonlinear and chaotic non-ideal vibrating system with shape memory alloy (SMA)". *Journal of Theoretical and Applied Mechanics* 46, 3, pp. 597-620.
- Piccirillo, V., Balthazar, J. M., Pontes Jr., B. R. and Felix, J. L. P., 2009. "Chaos control of a nonlinear oscillator with shape memory alloy (SMA) using optimal linear control: Part I: ideal energy source". *Nonlinear Dynamics*, vol. 55, Numbers 1-2, pp. 139-149.
- Piccirillo, V., Balthazar, J. M., Pontes Jr., B. R. and Felix, J. L. P., 2009. "Chaos control of a nonlinear oscillator with shape memory alloy (SMA) using optimal linear control: Part II: non-ideal energy source". *Nonlinear Dynamics*, vol. 56, number 3, pp. 243-253.
- Vakakis A.F., Gendelman, O.V., Bergman, L.A., MacFarland D.M., Kerscher G., Lee Y.S, 2008, "Nonlinear Target Energy Transfer in Mechanical and Structural Systems". Ed. Springer Verlag Holland, 800p.